Chemical Science

ROYAL SOCIETY OF CHEMISTRY

EDGE ARTICLE

View Article Online
View Journal | View Issue

Cite this: *Chem. Sci.*, 2023, **14**, 2652

All publication charges for this article have been paid for by the Royal Society of Chemistry

Received 21st December 2022
Accepted 5th February 2023

DOI: 10.1039/d2sc06982b

rsc.li/chemical-science

Tailoring the high-brightness "warm" white light emission of two-dimensional perovskite crystals *via* a pressure-inhibited nonradiative transition†

Yuanyuan Fang,[a] Jingtian Wang,[a] Long Zhang,[a] Guangming Niu,[b] Laizhi Sui,*[b] Guorong Wu,[b] Kaijun Yuan,[b] Kai Wang*[ac] and Bo Zou*[a]

Efficient warm white light emission is an ideal characteristic of single-component materials for light-emitting applications. Although two-dimensional hybrid perovskites are promising candidates for light-emitting diodes, as they possess broadband self-trapped emission and outstanding stability, they rarely achieve a high photoluminescence quantum yield of warm white light emissions. Here, an unusual pressure-induced warm white emission enhancement phenomenon from 2.1 GPa to 9.9 GPa was observed in two-dimensional perovskite $(2meptH_2)PbCl_4$, accompanied by a large increase in the relative quantum yield of photoluminescence. The octahedral distortions, accompanied with the evolution of organic cations, triggered the structural collapse, which caused the sudden emission enhancement at 2.1 GPa. Afterwards, the further intra-octahedral collapse promotes the formation of self-trapped excitons and the substantial suppression of nonradiative transitions are responsible for the continuous pressure-induced photoluminescence enhancement. This study not only clearly illustrates the relationship between crystal structure and photoluminescence, but also provides an experimental basis for the synthesis of high-quality warm white light-emitting 2D metal halide perovskite materials.

Introduction

Two-dimensional (2D) organic–inorganic hybrid perovskites have received tremendous attention for their diversity and stability compared to 3D perovskites.[1–6] Although a variety of 2D perovskites have been synthesized so far, further understanding the structure–property relationship of these 2D materials and improving their optical properties are essential for their practical applications. In particular, the development of white light-emitting perovskites always lags behind that of their green and red emission analogues, which limits their further application as single-component white light-emitting diodes (LEDs).[7–10] Recently, the "warm" white light-emitting perovskite $(2meptH_2)PbCl_4$ (2mept = 2-methyl-1,5-diaminopentane) has attracted our attention due to its potential to be used in indoor lighting applications (Fig. 1a).[11] However, it is plagued by a low photoluminescence (PL) efficiency of only 1.05% at room temperature. Its large Stokes shift and broadband emission are attributed to self-trapped excitons (STEs) (Fig. 1b). As is well known, STE emission derives from strong electron phonon coupling in the distorted crystal structure, which has great potential to be delicately modulated.

To date, numerous intriguing optical phenomena have been observed under extreme hydrostatic pressures by using diamond anvil cell (DAC) chamber design.[12–15] Therefore, pressure is regarded as a favourable method to adjust the crystal structure and physical properties without changing the chemical composition at finite pressures.[16–20] Indeed, many successful high-pressure experiments have been carried out on 3D perovskites, whereby pressure-driven phase transformation, bandgap modulation and metallization were achieved.[21–24] However, the developments of 3D materials upon compression are limited by the pressure-induced PL weakening. Over the past couple of years, more researchers have turned their attention to the study of low-dimensional perovskites.[25–29] Although the pressure-induced STE emission caused by stronger quantum confinement and site isolation in 0D Cs_4PbBr_6 and 1D $C_4N_2H_{14}SnBr_4$ and $C_4N_2H_{14}PbCl_4$ has been reported,[30–32] there is still little information about the pressure responses of STE emission in strictly 2D perovskites, especially warm white light-emitting perovskites.[33–35] Therefore, shedding light on the optical

[a]*State Key Laboratory of Superhard Materials, College of Physics, Jilin University, Changchun 130012, China. E-mail: kaiwang@jlu.edu.cn; zoubo@jlu.edu.cn*

[b]*State Key Laboratory of Molecular Reaction Dynamics, Dalian Institute of Chemical Physics, Chinese Academy of Sciences, 457 Zhongshan Road, Dalian 116023, China. E-mail: lzsui@dicp.ac.cn*

[c]*Shandong Key Laboratory of Optical Communication Science and Technology, School of Physics Science and Information Technology, Liaocheng University, Liaocheng 252000, China*

† Electronic supplementary information (ESI) available: Experimental details; high-pressure experimental data, including PL spectra, IR, Raman and UV-vis spectra; ADXRD pattern and structure refinement lattice constants; colour scale; colour temperature values; and pressure-dependent simulation results. See DOI: https://doi.org/10.1039/d2sc06982b

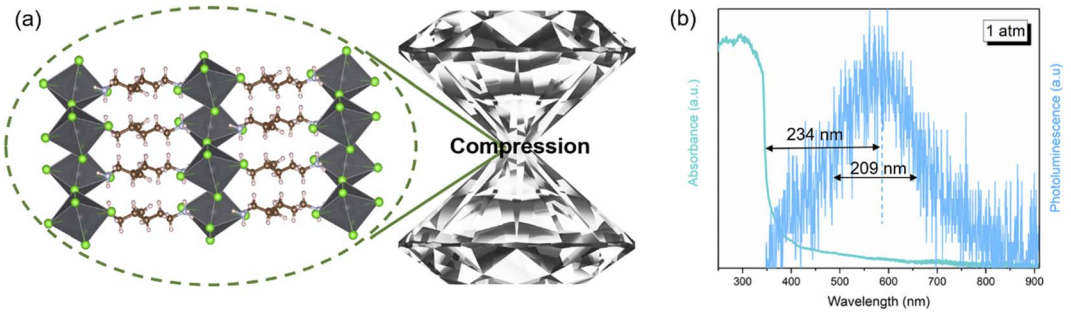

Fig. 1 (a) Ambient crystal structure of $(2meptH_2)PbCl_4$ and simple schematic diagram of the diamond anvil cell used for high pressure experiments. (b) Absorption (turquoise) and photoluminescence (deep sky-blue) spectra excited by 355 nm ultraviolet light of $(2meptH_2)PbCl_4$ crystals at ambient conditions.

property–crystal structure relationships of warm white light-emitting 2D metal halide perovskites remains a great challenge.

Here, by applying hydrostatic pressure on 2D $(2meptH_2)PbCl_4$ perovskite, a pressure-driven continuous warm white emission enhancement was successfully achieved. This breaks the long-standing status quo that pressure-induced lattice contraction typically results in high-brightness cool white emission from white light-emitting perovskite materials. Refined high-pressure X-ray diffraction data revealed that a sudden increase in the degree of structural distortion causes a significant increase in electron–phonon coupling energy, which promotes the formation and radiative recombination of STEs, resulting in an obvious photoluminescence enhancement of 2.1 GPa. With further compression up to 9.9 GPa, using the photoluminescence lifetime and relative photoluminescence quantum yield to estimate the nonradiative recombination rate of the crystal, it is concluded that the effective inhibition of nonradiative recombination by high pressure is the main reason for the emission enhancement. Our findings deepen our understanding of the structure–property relationship at high pressure and provide experimental clues for designing materials that emit high-intensity warm white light.

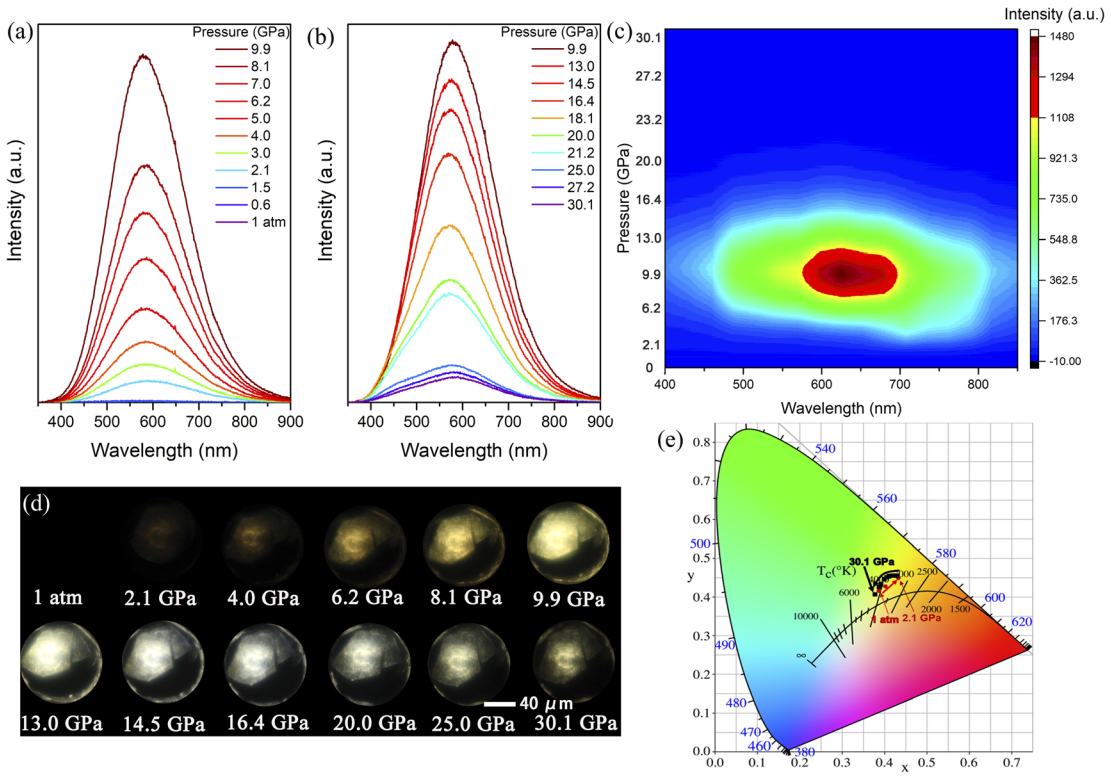

Fig. 2 (a and b) Pressure-induced evolution of emission spectra of $(2meptH_2)PbCl_4$ upon compression; (c) two-dimensional projection of the PL emission spectra under compression; (d) optical images at selected pressures under UV irradiation of 355 nm; (e) chromaticity coordinates of the emissions as a function of pressure. The pressure range from 1 atm to 2.1 GPa is represented by the crimson round dots, while the range of 3.0–30.1 GPa is represented by the black diamond dots.

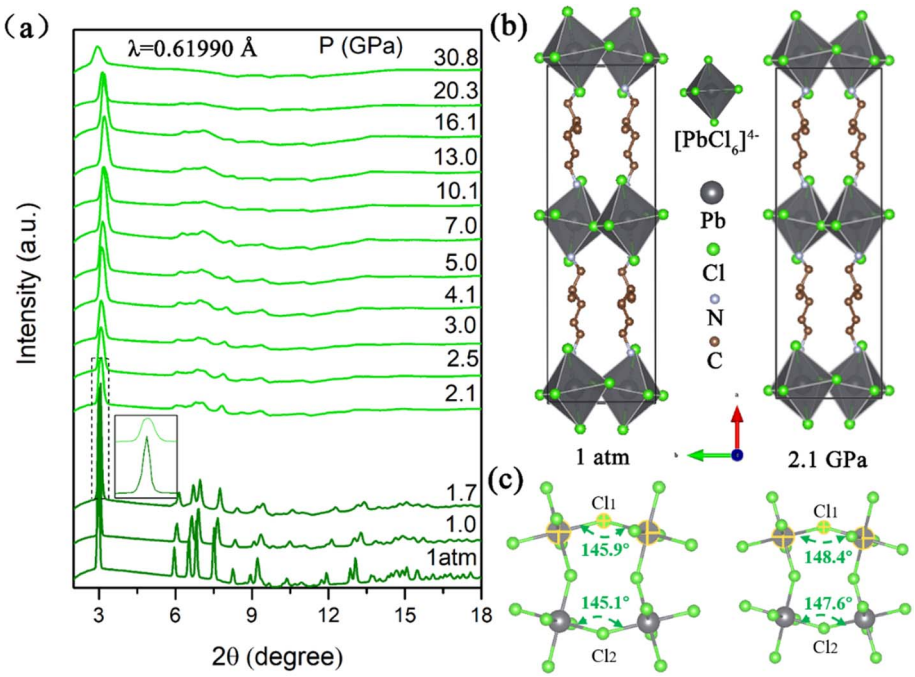

Fig. 3 (a) Representative *in situ* high-pressure ADXRD patterns of the $(2meptH_2)PbCl_4$ crystal. (b) Crystal structure of $(2meptH_2)PbCl_4$ perpendicular to the *c* axis. (c) Illustrations of the inorganic layer distortion at 1 atm and 2.1 GPa.

Results and discussion

When $(2meptH_2)PbCl_4$ is excited by 355 nm ultraviolet light at ambient conditions, it exhibits very weak PL intensity and its photoluminescence quantum yield is only 1.05%.[11] Its maximum emission peak is located at 580 nm, which is a broadband emission with a full width at half maximum of 209 nm spanning the whole visible spectrum. The Stokes shift of up to 234 nm indicates that this faint PL originates from a self-trapping emission (Fig. 1b). *In situ* PL measurements were performed to explore the regulation process of emission properties upon compression. The PL intensity of the sample remains unchanged until 1.5 GPa. Notably, a sharp 8-fold increase in PL intensity is observed at 2.1 GPa, which could be reproduced in repeat experiments (Fig. S1†). With the pressure increasing, the PL intensity drastically increases, with a maximum at 9.9 GPa (Fig. 2a and S2†). However, during further compression up to 30.1 GPa, the emission intensity of the sample gradually decreases, but even at 30.1 GPa, the PL intensity is still significantly higher than that at ambient conditions (Fig. 2b and c). The corresponding photomicrographs clearly demonstrate the changes in PL brightness and colour throughout the compression process (Fig. 2d). Colour temperature is a measure of colour that indicates how warm or cold a light source appears. Warm white light always has a colour temperature from 3000 K to 4000 K. Therefore, according to the Commission Internationale de L'Eclairage (CIE) 1931 standard colour matching functions, the sample maintains the "warm" white light emission with a relatively low correlated colour temperature around 4000 K and a high colour rendering index greater than 80 almost throughout the entire pressurization process (Fig. 2e and Table S1†). This high-performance single-component "warm" white light emission is rare, even in the study of atmospheric pressure synthesis of low-dimensional perovskites.[36,37]

The transition of emission characteristics upon compression is usually accompanied by structural evolution and the above experimental results indicate a structure transition of the $(2meptH_2)PbCl_4$ crystal; therefore, *in situ* high-pressure angle-dispersive X-ray diffraction (ADXRD) experiments were performed. The high-pressure XRD patterns of $(2meptH_2)PbCl_4$ are shown in Fig. 3a. It is found that, at 2.1 GPa, the first peak centred around $2\theta = 3.02°$, corresponding to the Bragg (200) reflection, suddenly weakens and broadens, accompanied by a significant passivation of the remaining diffractions (Fig. 3a). These observations suggest a sudden structural distortion. Above 2.1 GPa, all Bragg diffraction peaks continuously shift to a larger 2θ direction until 10.1 GPa, after which the main diffraction peak undergoes a stage of barely any change, attributed to the onset of the reduction of structural symmetry. At 30.8 GPa, this first diffraction peak shows an obvious shift to lower angles, suggesting dramatic structural distortion and closeness to the amorphous state.[38,39] Meanwhile, along with partial diffraction, peaks gradually broaden, weaken and finally disappear, and no new diffraction peaks appear during the whole compression process.

Rietveld refinement of high-pressure X-ray diffraction data reveals that $(2meptH_2)PbCl_4$ adopts a monoclinic *Cc* structure with lattice parameters $a = 24.14(3)$ Å, $b = 7.63(2)$ Å, $c = 7.83(2)$ Å, $\beta = 98.37(3)°$, $V = 1426.80(1)$ Å^3 at ambient conditions, consistent with the previously reported results (Fig. S3†).[11] When the pressure reaches 2.1 GPa, the lattice parameters of

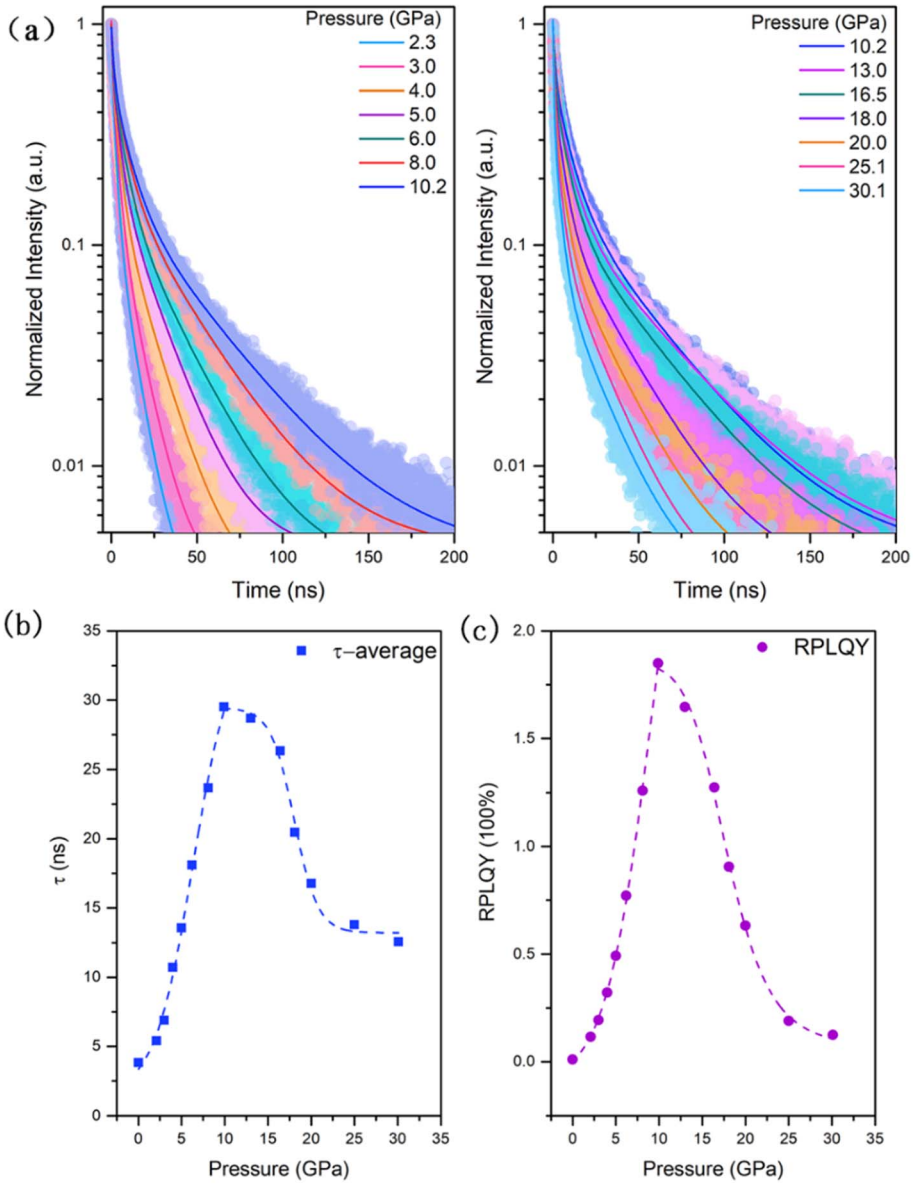

Fig. 4 (a) Normalized time-resolved PL decay curves of the $(2meptH_2)PbCl_4$ crystal at selected pressure. (b) Average PL lifetime of $(2meptH_2)PbCl_4$ as a function of pressure. (c) Evolution of estimated RPLQY during compression.

$(2meptH_2)PbCl_4$ change to $a = 23.29(1)$ Å, $b = 7.31(2)$ Å, $c = 7.68(2)$ Å, $\beta = 82.20(3)°$, $V = 1296.00(1)$ Å^3 (Fig. 3b). Structural analyses disclose that the compression of the crystal axis exhibits obvious anisotropy, which is related to the separation of inorganic octahedra by long-chain organic cations along the *a*-axis, so the compression of the *a*-axis is significantly accelerated (Fig. S4a†). Notably, at 2.1 GPa, the volume of the unit cell collapses significantly (Fig. S4b†). By fitting the unit-cell volume of the Birch–Murnaghan equation of state, the transition of the bulk elastic modulus *K* from 26.8 to 34.5 can be obtained, which are all typical characteristics of an isostructural phase transition, coinciding with the sudden enhancement of emission.[40] To determine how the distortion of the inorganic framework upon compression affects the organic cations in the structure, we also performed *in situ* high-pressure infrared absorption spectroscopy experiments to complement the high-pressure behaviour of organic cations (Fig. S5†). At 2.0 GPa, the peak of the infrared absorption spectrum is significantly weakened and broadened, indicating that the vibration of the organic cation is severely suppressed by the inorganic framework, corresponding to the sudden enhancement of the luminescence caused by the collapse of the unit cell volume at this time.[41]

Moreover, the degree of distortion of the crystal structure is quantitatively evaluated by the Pb–Cl bond lengths.

$$\Delta d = \frac{1}{6}\sum\left[\frac{d_n - d}{d}\right]^2$$

where d is the average length of the Pb–Cl bond, and d_n is the six independent Pb–Cl bond lengths. At ambient conditions, the average Pb–Cl–Pb angle is 145.5°, the average length of the

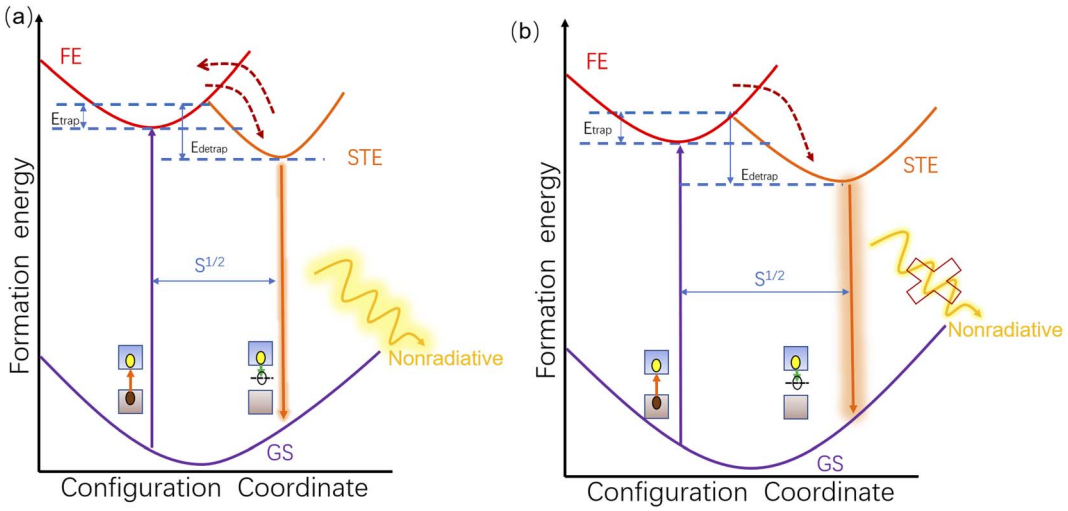

Fig. 5 (a and b) Illustration of the evolution of self-trapped exciton emission of the $(2meptH_2)PbCl_4$ crystal at ambient conditions and 5.0 GPa. GS: ground state; FE: free exciton state; STE: self-trapped exciton state, E_{trap}: exciton trapping activation energy, E_{detrap}: exciton detrapping activation energy, S: Huang–Rhys factor.

crystal Pb–Cl bond is 2.856 Å, and the Δd value is 1.354×10^{-5}, indicating that the $PbCl_6$ octahedral structure is slightly distorted (Fig. 3c). When the applied pressure reaches 2.1 GPa, the average Pb–Cl–Pb angle is 148.0°, the average Pb–Cl bond length in the crystal is 2.806 Å, and the Δd value reaches 3.660×10^{-3}, an increase in two orders of magnitude, indicating an extreme distortion of the $PbCl_6$ octahedral structure. The dramatic weakening or even disappearance of Raman peaks below 200 cm^{-1} also indicates a significant deformation of octahedral perovskites at 2.1 GPa (Fig. S6†). The more twisted $PbCl_6$ octahedral structure has a higher electron–phonon coupling energy, which promotes the formation of self-trapped excitons and radiative recombination emission, resulting in the sudden enhancement of PL intensity.[42–44]

To further identify the mechanism of the emission enhancement, time-resolved PL (TRPL) measurements were performed upon compression (Fig. 4a). Because the PL of the sample under ambient conditions is too weak to be tested, the TRPL was measured from 2.3 GPa when the PL intensity of the sample suddenly increases. During the pressurization process, the PL decay gradually slows down in the range from 2.3 GPa to 10.2 GPa. However, when the pressure is over 10.2 GPa, the PL shows a faster decay trend. This change trend is in line with the trend of steady-state spectral intensity increasing first and then decreasing around 10.0 GPa. The time resolved PL decays were fitted by the double exponential function $I(t) = I(0)\cdot[A_1 \exp(-t/\tau_1) + A_2 \exp(-t/\tau_2)]$, and mean PL lifetimes were calculated by $\langle\tau\rangle = [A_1\tau_1^2 + A_2\tau_2^2]/[A_1\tau_1 + A_2\tau_2]$. As shown in Fig. 4b, there is a significant increase in the mean lifetime upon compression below 10.2 GPa. Above 10.2 GPa, the mean PL lifetime becomes shorter, since in the self-trapped emitting materials, the fast component is usually assigned to nonradiative transitions, whereas the slow component is due to the radiative recombination of STEs.[45,46] Therefore, below 10.2 GPa, more radiative recombination causes an increase in PL intensity, and above 10.2 GPa more nonradiative transition channels appear, causing a quenching of the PL intensity. Combined with the test results of the high-pressure steady-state PL spectrum and transient PL spectrum, using the method of quantitative analysis of the relative quantum yield, which was first proposed by Dr Xujie Lü,[47] we also calculated the relative PL quantum yield (RPLQY) of $(2meptH_2)PbCl_4$ upon compression (Fig. 4c). The RPLQY increases first and then decreases before and after 10.2 GPa, which quantitatively proves that the pressure optimized the luminescence properties of the sample.

Furthermore, since in PL spectroscopy the relative quantum yield of PL and the PL lifetime are determined by the radiative decay rate (k_r) and the nonradiative decay rate (k_{nr}), according to the Jablonski energy level diagram, the RPLQY (Φ) and the PL lifetime can be expressed as

$$\Phi_{RPLQY} = \frac{k_r}{k_r + k_{nr}}$$

$$\tau = \frac{1}{k_r + k_{nr}}$$

Based on the estimated RPLQY and the test results of the average PL lifetime, it can be found that the k_r is slightly enhanced upon compression, but the change is not particularly obvious. At the same time, the k_{nr} is greatly reduced under pressure (Table S2†).

Summarizing the above analysis, the mechanism of photoluminescence enhancement of $(2meptH_2)PbCl_4$ under high pressure is shown in Fig. 5. As illustrated in Fig. 5a, because the inorganic framework is protected by large-sized organic cations, the crystal structure shrinks only slightly, resulting in a small degree of structural deformation and causing the weak electron–phonon coupling energy. Therefore, the energy difference between the free exciton state and the self-trapped exciton state

is limited, which improves the de-trapping ability of the self-trapped excitons, as indicated by the upward red arrow in Fig. 5a. Consequently, the PL of samples below 2.1 GPa is weak.[47] Upon further compression, the degree of distortion of the crystal structure increases significantly at 2.1 GPa, which is favourable for the formation of self-trapped excitons and the enhancement of the electron–phonon coupling of STEs.[11,46] Thus, the significant increase in PL intensity can be attributed to the radiative recombination promoted by the weakened self-detrapping ability of self-trapped excitons at 2.1 GPa. Furthermore, the phonon-assisted nonradiative recombination process of self-trapped excitons is greatly suppressed (Fig. 5b), resulting in a further significant enhancement of the PL of the $(2meptH_2)PbCl_4$ crystal until 9.9 GPa.[48,49] At pressures above 9.9 GPa, the distortion of the sample intensifies and the disordered stage starts, thus inhibiting the radiative recombination and promoting the nonradiative transition, and the PL begins to weaken at this time. In addition, the shape of the PL spectra always maintains obvious symmetry, indicating that multiple STE states with broad emission coexist well in equilibrium. Meanwhile, although the full width at half maximum (FWHM) of the emission band shows a slight decreasing trend (Fig. S8a†), the wide-range FWHM of more than 190 nm is always maintained within 30.1 GPa and the broadband emission of the sample always spans the whole range of the visible spectrum, which provides support for the sample to always maintain warm white light emission.

Conclusions

In summary, we have performed high-pressure experiments for tuning the optical properties and crystal structure of a white-emitting two-dimensional perovskite material $(2meptH_2)PbCl_4$ crystal. For samples with only weak PL at ambient conditions, there was a sudden increase in PL at 2.1 GPa, and the PL continued to increase until 9.9 GPa, after which it began to weaken. It is noteworthy that the sample maintained a rare warm white light emission throughout the pressurization process. By analysing the high-pressure synchrotron radiation X-ray diffraction data, the sample structure collapsed along the direction of the organic layer, and the degree of distortion in the crystal structure increased by two orders of magnitude at 2.1 GPa. This caused an increase in the detrapping activation energy of the structure, which promoted the radiative recombination of self-trapped excitons, resulting in a sudden PL enhancement of self-trapped emission at 2.1 GPa. With the further compression at 2.1 GPa–9.9 GPa, the lattice shrinkage rigidity enhanced and the pressure had a significant inhibitory effect on the nonradiative loss of self-trapped excitons, resulting in enhanced PL production. This work not only confirms that pressure is an effective method to enhance the quantum yield of 2D metal halide broadband white light emission, but also provides some insights into the microscopic mechanism of the emission enhancement of self-trapped excitons at high pressure. It is hoped that these findings can provide an experimental basis for developing the design of future efficient white light metal halide materials for use in light-emitting devices.

Data availability

Essential data are provided in the main text and the ESI.† Additional data can be available from the corresponding author upon reasonable request.

Author contributions

Y. F., J. W., and L. Z. performed high pressure optical and XRD experiments. G. N., L. S., G. W., and K. Y. carried out the time-resolved PL decay dynamics measurements. Y. F., K. W., and B. Z. wrote the manuscript. All authors discussed and commented on the manuscript.

Conflicts of interest

There are no conflicts to declare.

Acknowledgements

This work was supported by the National Natural Science Foundation of China (NSFC) (No. 12204190, 21725304, 12174146), the China Postdoctoral Science Foundation (No. 2022M721322), the fundamental research funds for the Central Universities, the Chemical Dynamics Research Center (No. 21688102), the Key Technology Team of the Chinese Academy of Sciences (No. GJJSTD20190002), and the Special Construction Project Fund for Shandong Province Taishan Scholars. ADXRD experiments were mainly performed at 4W2 HP-Station, Beijing Synchrotron Radiation Facility (BSRF).

Notes and references

1 F. O. Saouma, C. C. Stoumpos, J. Wong, M. G. Kanatzidis and J. I. Jang, *Nat. Commun.*, 2017, **8**, 742.
2 L. Mao, C. C. Stoumpos and M. G. Kanatzidis, *J. Am. Chem. Soc.*, 2019, **141**, 1171–1190.
3 E. Shi, B. Yuan, S. B. Shiring, Y. Gao, A. Akriti, Y. Guo, C. Su, M. Lai, P. Yang, J. Kong, B. M. Savoie, Y. Yu and L. Dou, *Nature*, 2020, **580**, 614–620.
4 S. Kahmann, H. Duim, H. H. Fang, M. Dyksik, S. Adjokatse, M. Rivera Medina, M. Pitaro, P. Plochocka and M. A. Loi, *Adv. Funct. Mater.*, 2021, **31**, 2103778.
5 M. Kober-Czerny, S. G. Motti, P. Holzhey, B. Wenger, J. Lim, L. M. Herz and H. J. Snaith, *Adv. Funct. Mater.*, 2022, **32**, 2203064.
6 P. P. Sun, D. R. Kripalani, W. Chi, S. A. Snyder and K. Zhou, *Mater. Today*, 2021, **47**, 45–52.
7 S. Kahmann, E. K. Tekelenburg, H. Duim, M. E. Kamminga and M. A. Loi, *Nat. Commun.*, 2020, **11**, 2344.
8 K. Ji, M. Anaya, A. Abfalterer and S. D. Stranks, *Adv. Optical Mater.*, 2021, **9**, 2002128.
9 J. Jiang, Z. Chu, Z. Yin, J. Li, Y. Yang, J. Chen, J. Wu, J. You and X. Zhang, *Adv. Mater.*, 2022, **34**, e2204460.
10 N. Yukta and S. Satapathi, *ACS Appl. Electron. Mater.*, 2022, **4**, 1469–1484.

11 S. Wang, Y. Yao, Z. Wu, Y. Peng, L. Li and J. Luo, *J. Mater. Chem. C*, 2018, **6**, 12267–12272.
12 G. Liu, L. Kong, W. Yang and H. K. Mao, *Mater. Today*, 2019, **27**, 91–106.
13 Y. Shang, Z. Liu, J. Dong, M. Yao, Z. Yang, Q. Li, C. Zhai, F. Shen, X. Hou, L. Wang, N. Zhang, W. Zhang, R. Fu, J. Ji, X. Zhang, H. Lin, Y. Fei, B. Sundqvist, W. Wang and B. Liu, *Nature*, 2021, **599**, 599–604.
14 Y. Yin, W. Tian, H. Luo, Y. Gao, T. Zhao, C. Zhao, J. Leng, Q. Sun, J. Tang, P. Wang, Q. Li, X. Lü, J. Bian and S. Jin, *ACS Energy Lett.*, 2021, **7**, 154–161.
15 X. Lü, C. Stoumpos, Q. Hu, X. Ma, D. Zhang, S. Guo, J. Hoffman, K. Bu, X. Guo, Y. Wang, C. Ji, H. Chen, H. Xu, Q. Jia, W. Yang, M. G. Kanatzidis and H. K. Mao, *Natl. Sci. Rev.*, 2021, **8**, nwaa288.
16 Q. Wang, D. Li, G. Cao, Q. Shi, J. Zhu, M. Zhang, H. Cheng, Q. Wen, H. Xu, L. Zhu, H. Zhang, R. J. Perry, O. Spadaro, Y. Yang, S. He, Y. Chen, B. Wang, G. Li, Z. Liu, C. Yang, X. Wu, L. Zhou, Q. Zhou, Z. Ju, H. Lu, Y. Xin, X. Yang, C. Wang, Y. Liu, G. I. Shulman, V. D. Dixit, L. Lu, H. Yang, R. A. Flavell and Z. Yin, *Nature*, 2021, **600**, 314–318.
17 L. Ma, K. Wang, Y. Xie, X. Yang, Y. Wang, M. Zhou, H. Liu, X. Yu, Y. Zhao, H. Wang, G. Liu and Y. Ma, *Phys. Rev. Lett.*, 2022, **128**, 167001.
18 Z. Zeng, J. Wen, H. Lou, X. Zhang, L. Yang, L. Tan, B. Cheng, X. Zuo, W. Yang, W. L. Mao, H. K. Mao and Q. Zeng, *Nature*, 2022, **608**, 513–517.
19 Z. Zhang, T. Cui, M. J. Hutcheon, A. M. Shipley, H. Song, M. Du, V. Z. Kresin, D. Duan, C. J. Pickard and Y. Yao, *Phys. Rev. Lett.*, 2022, **128**, 047001.
20 K. Bu, Q. Hu, X. Qi, D. Wang, S. Guo, H. Luo, T. Lin, X. Guo, Q. Zeng, Y. Ding, F. Huang, W. Yang, H. K. Mao and X. Lü, *Nat. Commun.*, 2022, **13**, 4650.
21 L. Wang, K. Wang and B. Zou, *J. Phys. Chem. Lett.*, 2016, **7**, 2556–2562.
22 G. Liu, L. Kong, J. Gong, W. Yang, H. K. Mao, Q. Hu, Z. Liu, R. D. Schaller, D. Zhang and T. Xu, *Adv. Funct. Mater.*, 2017, **27**, 1604208.
23 Q. Li, Y. Wang, W. Pan, W. Yang, B. Zou, J. Tang and Z. Quan, *Angew. Chem., Int. Ed. Engl.*, 2017, **56**, 15969–15973.
24 J. Jiang, G. Niu, L. Sui, X. Wang, Y. Zhang, L. Che, G. Wu, K. Yuan and X. Yang, *J. Phys. Chem. Lett.*, 2021, **12**, 7285–7292.
25 Z. Li, B. Jia, S. Fang, Q. Li, F. Tian, H. Li, R. Liu, Y. Liu, L. Zhang, S. F. Liu and B. Liu, *Adv. Sci.*, 2022, 2205837, DOI: **10.1002/advs.202205837**.
26 L. Li, W. Wu, D. Li, C. Ji, S. Lin, M. Hong and J. Luo, *CCS Chem.*, 2022, **4**, 2491–2497.
27 W. Wu, X. Shang, Z. Xu, H. Ye, Y. Yao, X. Chen, M. Hong, J. Luo and L. Li, *Adv. Sci.*, 2023, 2206070, DOI: **10.1002/advs.202206070**.
28 S. Guo, Y. Li, Y. Mao, W. Tao, K. Bu, T. Fu, C. Zhao, H. Luo, Q. Hu, H. Zhu, E. Shi, W. Yang, L. Dou and X. Lü, *Sci. Adv.*, 2022, **8**, eadd1984.
29 T. Yin, H. Yan, I. Abdelwahab, Y. Lekina, X. Lü, W. Yang, H. Sun, K. Leng, Y. Cai, Z. X. Shen and K. P. Loh, *Nat. Commun.*, 2023, **14**, 411.
30 Z. Ma, Z. Liu, S. Lu, L. Wang, X. Feng, D. Yang, K. Wang, G. Xiao, L. Zhang, S. A. T. Redfern and B. Zou, *Nat. Commun.*, 2018, **9**, 4506.
31 Y. Shi, Z. Ma, D. Zhao, Y. Chen, Y. Cao, K. Wang, G. Xiao and B. Zou, *J. Am. Chem. Soc.*, 2019, **141**, 6504–6508.
32 Y. Fang, T. Shao, L. Zhang, L. Sui, G. Wu, K. Yuan, K. Wang and B. Zou, *JACS Au*, 2021, **1**, 459–466.
33 S. Liu, S. Sun, C. Gan, A. Águila, Y. Fang, J. Xing, T. Do, T. White, H. Li, W. Huang and Q. Xiong, *Sci. Adv.*, 2019, **5**, eaav9445.
34 T. Yin, B. Liu, J. Yan, Y. Fang, M. Chen, W. K. Chong, S. Jiang, J. L. Kuo, J. Fang, P. Liang, S. Wei, K. P. Loh, T. C. Sum, T. J. White and Z. X. Shen, *J. Am. Chem. Soc.*, 2019, **141**, 1235–1241.
35 S. Guo, Y. Zhao, K. Bu, Y. Fu, H. Luo, M. Chen, M. P. Hautzinger, Y. Wang, S. Jin, W. Yang and X. Lü, *Angew. Chem., Int. Ed. Engl.*, 2020, **59**, 17533–17539.
36 X. Li, S. Wang, S. Zhao, L. Li, Y. Li, B. Zhao, Y. Shen, Z. Wu, P. Shan and J. Luo, *Chemistry*, 2018, **24**, 9243–9246.
37 Y. Han, J. Yin, G. Cao, Z. Yin, Y. Dong, R. Chen, Y. Zhang, N. Li, S. Jin, O. F. Mohammed, B. B. Cui and Q. Chen, *ACS Energy Lett.*, 2021, **7**, 453–460.
38 X. Zhan, X. Jiang, P. Lv, J. Xu, F. Li, Z. Chen and X. Liu, *Angew. Chem., Int. Ed. Engl.*, 2022, **61**, e202205491.
39 S. Guo, K. Bu, J. Li, Q. Hu, H. Luo, Y. He, Y. Wu, D. Zhang, Y. Zhao, W. Yang, M. G. Kanatzidis and X. Lü, *J. Am. Chem. Soc.*, 2021, **143**, 2545–2551.
40 L. Wang, K. Wang, G. Xiao, Q. Zeng and B. Zou, *J. Phys. Chem. Lett.*, 2016, **7**, 5273–5279.
41 Y. Gu, K. Wang, Y. Dai, G. Xiao, Y. Ma, Y. Qiao and B. Zou, *J. Phys. Chem. Lett.*, 2017, **8**, 4191–4196.
42 S. Wang, Y. Yao, J. Kong, S. Zhao, Z. Sun, Z. Wu, L. Li and J. Luo, *Chem. Commun.*, 2018, **54**, 4053–4056.
43 X. Huang, X. Li, Y. Tao, S. Guo, J. Gu, H. Hong, Y. Yao, Y. Guan, Y. Gao, C. Li, X. Lü and Y. Fu, *J. Am. Chem. Soc.*, 2022, **144**, 12247–12260.
44 R. Wu, Y. Liu, S. Hu, P. Fu and Z. Xiao, *Adv. Optical Mater.*, 2022, **10**, 2201081.
45 B. Yang and K. Han, *J. Phys. Chem. Lett.*, 2021, **12**, 8256–8262.
46 X. Cheng, Z. Xie, W. Zheng, R. Li, Z. Deng, D. Tu, X. Shang, J. Xu, Z. Gong, X. Li and X. Chen, *Adv. Sci.*, 2022, **9**, 2103724.
47 Y. Wang, S. Guo, H. Luo, C. Zhou, H. Lin, X. Ma, Q. Hu, M. H. Du, B. Ma, W. Yang and X. Lü, *J. Am. Chem. Soc.*, 2020, **142**, 16001–16006.
48 X. Meng, S. Ji, Q. Wang, X. Wang, T. Bai, R. Zhang, B. Yang, Y. Li, Z. Shao, J. Jiang, K. L. Han and F. Liu, *Adv. Sci.*, 2022, **9**, 2203596.
49 H. Luo, S. Guo, Y. Zhang, K. Bu, H. Lin, Y. Wang, Y. Yin, D. Zhang, S. Jin, W. Zhang, W. Yang, B. Ma and X. Lü, *Adv. Sci.*, 2021, **8**, e2100786.